

人のゲノムコピー数変化(CNVs). 次世代シーケンサー現場の会第三回研究会, 2013年9月4-5日, 神戸 (ポスター発表)

Kosho T, Yue F, Saka S, Tsumita N, Kasahara Y, Okada T, Mizumoto S, Kobayashi M, Nakayama J, Miyake N, Nomura Y, Era T, Hatamochi A, Fukushima F, Matsumoto N, Sugahara K, Sasaki K, Takeda S. Establishment and validation of iPS cells and knockout mice for dermatan 4-O-sulfotransferase 1 (D4ST1)-deficient Ehlers-Danlos syndrome (DDEDS). American Society of Human Genetics, 2013年10月22-26日, Boston

H. 知的財産権の出願・登録状況

1. 特許取得

なし

2. 実用新案登録

なし

3. その他

なし

研究成果の刊行に関する一覧表

書籍

著者氏名	論文タイトル名	書籍全体の編集者名	書籍名	出版社名	出版地	出版年	ページ

雑誌

発表者氏名	論文タイトル名	発表誌名	巻号	ページ	出版年
Tsurusaki Y, et al., Matsumoto N.	Exome sequencing identifies an <i>OFDI</i> mutation in a family of X-linked lethal congenital malformation syndrome: delineation of male Oral-facial-digital syndrome type 1.	Clin Genet	83 (2)	135-144	2013
Tsurusaki Y, et al., Matsumoto N.	The diagnostic utility of exome sequencing in Joubert syndrome related disorders.	J Hum Genet	58(2)	113-115	2013
Kondo Y, et al., Matsumoto N.	Whole-exome sequencing identified a homozygous <i>FNBP4</i> mutation in a family with a condition microphthalmia with limb anomalies-like	Am J Med Genet Part A	161A	1543-1546	2013
Miyake N, et al., Matsumoto N.	Mitochondrial complex III deficiency caused by a homozygous <i>UQCRC2</i> mutation presenting with neonatal-onset recurrent metabolic decompensation.	Hum Mut	34(3)	446-452	2013
Saito H, et al., Matsumoto N.	<i>De novo</i> mutations in the autophagy gene <i>WDR45</i> cause static encephalopathy of childhood with neurodegeneration in adulthood.	Nat Genet	45(4)	445-449	2013

Kondo Y, et al., Matsumoto N.	Pathogenic mutations in two families with congenital cataract identified by whole-exome sequencing.	Mol Vis	19	384-389	2013
Nakamura K, et al., Matsumoto N, Saitsu H.	Clinical spectrum of <i>SCN2A</i> mutations expanding to Ohtahara syndrome.	Neurology	81(11)	992-998	2013
Koshimizu E, et al., Matsumoto N.	Exome sequencing identifies an <i>OFDI</i> mutation in a family of X-linked lethal congenital malformation syndrome: delineation of male Oral-facial-digital syndrome type 1.	Plos One	8(9)	e74167	2013
Nakajima M, et al., Matsumoto N, et al..	Mutations in <i>B3GALT6</i> , which encodes a glycosaminoglycan linker region enzyme, cause a spectrum of skeletal and connective tissue disorders.	Am J Hum Genet	92(6)	927-934	2013
Iida A, et al., Matsumoto N, Ikegawa S.	Exome sequencing identifies a novel <i>INPPL1</i> mutation in opsismodysplasia.	J Hum Genet	58(6)	391-394	2013
Nishiguchi KM, et al., Matsumoto N, et al.	Whole genome sequencing in patients with retinitis pigmentosa reveals pathogenic DNA structural changes and <i>NEK2</i> as a new disease gene.	Proc Natl Acad Sci USA	110(40)	16139-16144	2013
Kodera H, et al., Matsumoto N, Saitsu H.	Target capture sequencing for detection of mutations and copy number changes causing early-onset epileptic encephalopathy.	Epilepsia	54(7)	1262-1269	2013

Ravenscroft G, et al., Matsumoto N*, Laing N (*: co-correspondence and last authros)	Mutations in KLHL40 are a frequent cause of severe autosomal-recessive nemaline myopathy.	Am J Hum Genet	93(1)	6-18	2013
Miyake N, et al., Matsumoto N, Niikawa N.	MLL2 and KDM6A mutations and their clinical consequences in Kabuki syndrome.	Am J Med Genet Part A	161(9)	2234-2243	2013
Nakamura K, et al., Matsumoto N, Saitsu H.	De novo mutations in GNAO1 encoding a Gαo subunit of heterotrimeric G proteins, cause epileptic encephalopathy.	Am J Hum Genet	93(3)	496-505	2013
Kodera H, et al., Matsumoto N, Saitsu H.	De novo mutations in SLC35A2 encoding a UDP-galactose transporter cause early-onset epileptic encephalopathy.	Hum Mut	34(12)	1708-1714	2013
Ohba C, et al., Matsumoto N, Saitsu H.	Diagnostic utility of whole exome sequencing in cerebellar atrophy in childhood.	Neurogenet	14 (3-4)	225-232	2013
Gupta VA, et al., Matsumoto N, et al.	Identification of KLHL41 mutations implicates BTB-Kelch-mediated ubiquitination as an alternate pathway to myofibrillar disruption in nemaline myopathy.	Am J Hum Genet	93(6)	1108-1117	2013
Nakajima J, et al., Matsumoto N, Miyake N.	A novel homozygous YARS2 mutation causes severe myopathy, lactic acidosis, and sideroblastic anemia syndrome.	J Hum Genet	58(12)	822-824	2013



Original Article

Exome sequencing in a family with an X-linked lethal malformation syndrome: clinical consequences of hemizygous truncating *OFD1* mutations in male patients

Tsurusaki Y, Kosho T, Hatasaki K, Narumi Y, Wakui K, Fukushima Y, Doi H, Saitsu H, Miyake N, Matsumoto N. Exome sequencing in a family with an X-linked lethal malformation syndrome: clinical consequences of hemizygous truncating *OFD1* mutations in male patients. Clin Genet 2013; 83: 135–144. © John Wiley & Sons A/S. Published by Blackwell Publishing Ltd, 2012

Oral-facial-digital syndrome type 1 (OFD1; OMIM #311200) is an X-linked dominant disorder, caused by heterozygous mutations in the *OFD1* gene and characterized by facial anomalies, abnormalities in oral tissues, digits, brain, and kidney; and male lethality in the first or second trimester pregnancy. We encountered a family with three affected male neonates having an ‘unclassified’ X-linked lethal congenital malformation syndrome. Exome sequencing of entire transcripts of the whole X chromosome has identified a novel splicing mutation (c.2388+1G > C) in intron 17 of *OFD1*, resulting in a premature stop codon at amino acid position 796. The affected males manifested severe multisystem complications in addition to the cardinal features of OFD1 and the carrier female showed only subtle features of OFD1. The present patients and the previously reported male patients from four families (clinical OFD1; Simpson-Golabi-Behmel syndrome, type 2 with an *OFD1* mutation; Joubert syndrome-10 with *OFD1* mutations) would belong to a single syndrome spectrum caused by truncating OFD1 mutations, presenting with craniofacial features (macrocephaly, depressed or broad nasal bridge, and lip abnormalities), postaxial polydactyly, respiratory insufficiency with recurrent respiratory tract infections in survivors, severe mental or developmental retardation, and brain malformations (hypoplasia or agenesis of corpus callosum and/or cerebellar vermis and posterior fossa abnormalities).

Conflict of interest

The authors have no conflict of interest to declare.

**Y Tsurusaki^{a*}, T Kosho^{b*},
K Hatasaki^c, Y Narumi^b,
K Wakui^b, Y Fukushima^b,
H Doi^a, H Saitsu^a, N Miyake^a
and N Matsumoto^a**

^aDepartment of Human Genetics, Yokohama City Graduate School of Medicine, Yokohama, Japan,

^bDepartment of Medical Genetics, Shinshu University School of Medicine, Matsumoto, Japan, and ^cDepartment of Pediatrics, Toyama Prefectural Central Hospital, Toyama, Japan

*These authors contributed equally to this work.

Key words: exome sequencing – *OFD1* – *OFD1* gene – splicing mutation – X-linked congenital malformation syndrome

Corresponding authors: Tomoki Kosho, MD, Department of Medical Genetics, Shinshu University School of Medicine, 3-1-1 Asahi, Matsumoto, Nagano 390-8621, Japan.

Tel.: +81 263 37 2618;

fax: +81 263 37 2619;

e-mail: ktomoki@shinshu-u.ac.jp

and

Naomichi Matsumoto, MD, PhD, Department of Human Genetics, Yokohama City Graduate School of Medicine, 3-9 Fukuura, Kanazawa-ku, Yokohama 236-0004, Japan.

Tel.: +81 45 787 260;

fax: +81 45 786 5219;

e-mail: naomat@yokohama-cu.ac.jp

Received 14 January 2012, revised and accepted for publication 26 March 2012

Oral-facial-digital syndrome type 1 (OFD1; OMIM #311200), originally described by Papillon-Leage and Psaume (1) and further delineated by Gorlin and Psaume (2), is an X-linked dominant developmental disorder with an estimated prevalence of 1:50,000, caused by mutations in the *OFD1* gene (OMIM #300170) (3–5). The disorder is characterized by facial anomalies and abnormalities in oral tissues, digits, brain and kidney (5). Almost all affected individuals with OFD1 are female, with highly variable expression, possibly resulting from random X inactivation (6). Affected males are generally lost in the first or second trimester of pregnancy (4). To date, only one liveborn male case with clinically definite OFD1 and a normal karyotype has been reported; the patient was born at 34 weeks of gestation and died 21 h after birth due to heart failure (7). In this report, we describe a family with three affected male neonates having an ‘unclassified’ X-linked lethal congenital malformation syndrome. Exome sequencing of entire transcripts of the whole X chromosome has successfully identified a causative splicing mutation in *OFD1*.

Subjects and methods

Clinical report

II-2, a 22-year-old woman, was referred to our clinic for genetic counseling (Fig. 1). Her deceased brother (II-4) had severe multiple congenital abnormalities. She had two sons (III-1 and III-5) with similar congenital abnormalities and a healthy boy (III-3) as well as two miscarriages (III-2, artificial; III-4, spontaneous). During genetic counseling and molecular investigations, she had another healthy boy (III-5). After identification of a heterozygous *OFD1* mutation, she was examined for features of OFD1. Only a few accessory frenulae and irregular teeth with no facial anomalies or tongue abnormalities were observed (Fig. 2a–e). A radiograph of her hands showed no abnormalities (Fig. 2f) and an abdominal ultrasonography detected no cysts in the kidneys, liver, or pancreas (data not shown). I-2, allegedly, had no apparent malformations or complications including renal diseases.

II-4 was born by caesarean section because of placental abruption at 33 weeks of gestation. Pregnancy was complicated by polyhydramnios. Apgar score was 3 at 1 min. His birth weight was 2056 g (+0 SD), length was 45.0 cm (+0.5 SD), and occipitofrontal circumference (OFC) was 34.0 cm (+2.0 SD). He manifested severe respiratory insufficiency and was transferred to a neonatal intensive care unit (NICU). His craniofacial features included a prominent forehead, a large fontanelle (5 × 5 cm), a low posterior hair-line, microphthalmia, hypertelorism, short palpebral fissures, depressed nasal bridge, low-set ears, a small cleft lip and a soft cleft palate, narrowing of the tip of the tongue, and a hypoplastic gum (Fig. 2g). Additional physical features included redundant neck skin, postaxial polydactyly of the left hand (Fig. 2h), wide halluces (Fig. 2i), micropenis, and left cryptorchidism.

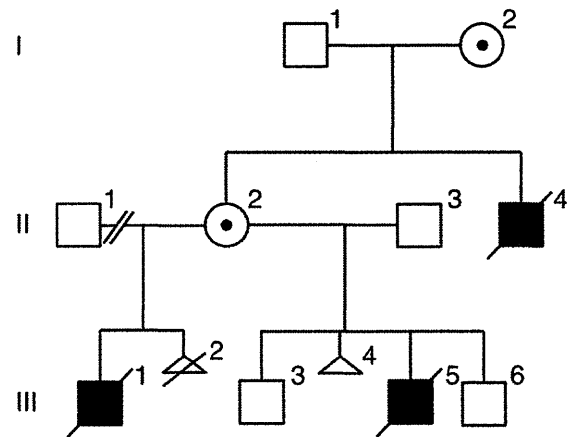


Fig. 1. Familial pedigree.

Ultrasonography revealed hypoplastic gyri, an atrial septal defect, and patent ductus arteriosus. Ophthalmological examination detected microcornea and retinal detachment. Intubation was impossible because of laryngeal anomalies and the patient died 11 h after birth. Additional autopsy findings included partial atelectasis and bilateral hydronephroses.

III-1 was delivered by emergency caesarean section at 39 weeks of gestation. Pregnancy was complicated by polyhydramnios and intrauterine growth retardation, with moderate macrocephaly. His birth weight was 3064 g (+0.1 SD). He was admitted to a NICU because of respiratory insufficiency, and received mechanical ventilation. His craniofacial features included microphthalmia, hypertelorism, short palpebral fissures, epicanthus, low-set ears, and a cleft lip and palate. Additional physical features included bilateral polydactyly of hands (postaxial) and feet (preaxial), and an ectopic urethral opening. Ultrasonography revealed hydrocephalus, agenesis of the corpus callosum and cerebellar vermis, and a complete atrioventricular septal defect. Ophthalmological examination detected persistent pupillary membrane and optic disc coloboma. G-banded chromosomes were normal (46,XY). The patient died at age 14 days due to heart failure.

III-5 was delivered by caesarean section at 32 weeks of gestation. Pregnancy was complicated by polyhydramnios, intrauterine growth retardation, and congenital heart defects. His birth weight was 1704 g (–0.2 SD), length was 40.0 cm (–0.8 SD), and OFC was 33.3 cm (+2.0 SD). He was admitted to a NICU because of respiratory insufficiency, and received mechanical ventilation. His craniofacial features included a prominent forehead, hypertelorism, dysplastic ears, a small cleft lip, and a soft cleft palate (Fig. 2j,k). Ultrasonography revealed hydrocephalus with Dandy-Walker malformation and hypoplastic left heart syndrome. G-banded chromosomes were normal (46,XY). The patient died 1 day after birth. Additional autopsy findings included agenesis of the cerebellar vermis (Fig. 2l), enlargement of the fourth ventricle and aqueduct, anomalous positioning of the esophagus, mild

Exome sequencing in a family with an X-linked lethal malformation syndrome

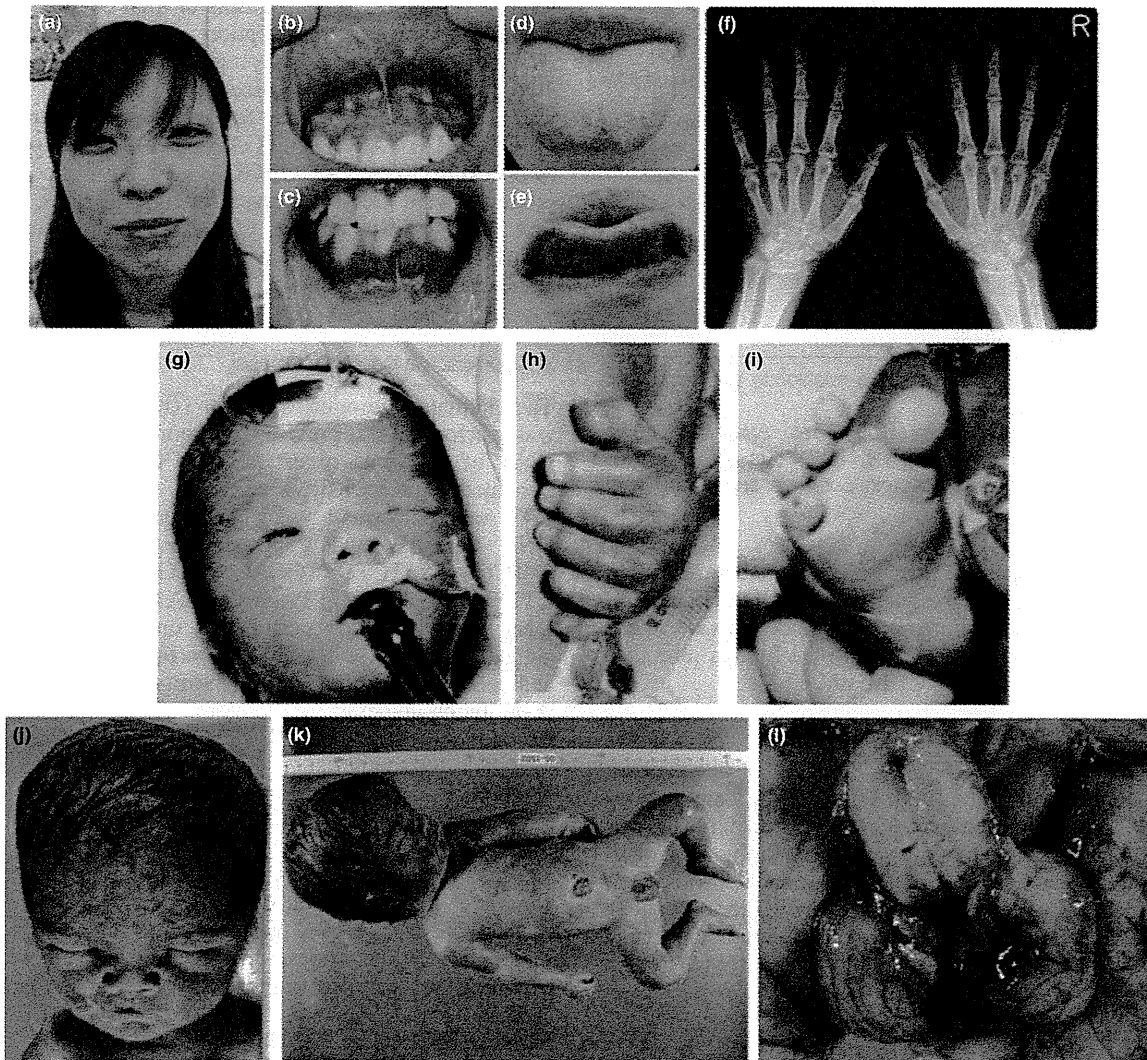


Fig. 2. Clinical photographs of II-2 (a–f), II-4 (g–i), and III-5 (j–l).

pulmonary congestion, and insufficient lobulation of the right lung.

The three affected male neonates, having strikingly similar clinical manifestations (Table 1), are considered to have had a congenital malformation syndrome with X-linked inheritance. Array-CGH analysis using 4200 BAC clones identified no pathologic genomic copy number abnormalities. Direct sequencing of *MID*, performed because of a partial similarity to these neonates' syndrome to X-linked Opitz-G/BBB syndrome (OMIM #300000) (8), revealed no mutation.

Library preparation

Genomic DNA for II-2, II-3, III-3, and III-6 was extracted from peripheral blood using the Genra PureGene Blood Kit (QIAGEN, Hilden, Germany), and genomic DNA for III-5 was extracted from the preserved dried umbilical cord using the DNeasy Blood

& Tissue Kit (QIAGEN). Three micrograms of high-quality (absorbance at 260 nm/absorbance at 280 nm: 1.8–2.0) genomic DNA from II-2 was fragmented using the Covaris model S2 system (Covaris, Woburn, MA). The target peak size was 150 bp. After the size of sheared DNA was checked using an Agilent 2100 Bioanalyzer (Agilent Technologies, Santa Clara, CA), adapter sequences were ligated to the ends of DNA fragments, and amplified according to the manufacturer's protocol (Agilent Technologies).

Exome capture and next-generation sequencing

Library DNA was hybridized for 24 h at 65°C using the SureSelect Human X Chromosome Demo Kit (Agilent Technologies). Captured DNA was diluted to a concentration of 8 pM and sequenced on a Genome Analyzer Ix (Illumina, San Diego, CA) with 76-bp paired-end reads. We used only one of the eight lanes in the flow

Table 1. Variant priority scheme after exome sequencing^a

	NEXTGENE	II-2	MAQ (SEATTLESEQ)
Total variants called	22,176	—	58,081
Chr X	3441	—	4383
Unknown SNP variants (dbSNP131, 1000 genomes)	910	—	882
Overlap of NEXTGENE and MAQ	—	169	—
NS/SS	—	17	—
Except for variants at segmental duplications	—	15	—

NS, non-synonymous; SNP, single-nucleotide polymorphism; SS, splice site (± 2).

^aMAQ was annotated with SEATTLESEQ ANNOTATION. The annotation includes gene names, dbSNP rs ID, and SNP functions (e.g. missense), protein positions and amino acid changes.

cell for II-2 (Illumina). Image analyses and base calling were performed using sequence control software real-time analysis and OFFLINE BASECALLER software v1.8.0 (Illumina). Reads were aligned to the human reference genome (UCSC hg19, NCBI build 37.1).

Mapping strategy and variant annotation

The quality-controlled (Path Filter) reads were mapped to the human reference genome (UCSC hg19, NCBI build 37.1), using mapping and assembly with quality (MAQ) and NEXTGENE software v2.0 (SoftGenetics, State College, PA). Single-nucleotide polymorphisms in MAQ-passed reads were annotated using the SEATTLESEQ ANNOTATION website (<http://gvs.gs.washington.edu/SeattleSeqAnnotation/>).

Priority scheme and capillary sequencing

Called variants found by each informatics method were filtered in terms of location on chromosome X, unregistered variants (excluding registered dbSNP131 and 1000 Genomes), overlapping variants called in common by NEXTGENE and MAQ, and non-synonymous changes and splice-site mutations (± 2 bp from exon-intron junctions) (Table 1). The variants were confirmed as true positives by Sanger sequencing of polymerase chain reaction (PCR) products amplified using genomic DNA as a template, except for variants within genes at segmental duplications. Sanger sequencing was performed on an ABI3500xl or ABI3100 autosequencer (Life Technologies, Carlsbad, CA). Sequencing data were analyzed using SEQUENCHER software (Gene Codes Corporation, Ann Arbor, MI).

Reverse transcription-PCR

Total RNA was isolated from EBV-transformed lymphoblastoid cell line (EBV-LCL) derived from II-2 and healthy control subjects using the RNeasy Plus Mini

Kit (QIAGEN). Five micrograms of total cellular RNA was used for reverse transcription with the Super Script III First-Strand Synthesis System (Life Technologies). Two microliters of synthesized complementary DNA was used for PCR with the following primers: ex17-F (5'-CTACCATCACCCACTGAGTC-3') and ex19-R (5'-TGAGACATATCCCCGGCAG-3'). Amplified PCR products were electrophoresed in agarose gels, purified from gels using the QIAquick Gel Extraction Kit (QIAGEN), cloned into pCR4-TOPO vector (Life Technologies) and sequenced.

X-chromosome inactivation assay

The human androgen receptor (HUMARA) assay was performed as previously reported (9). Genomic DNA of II-2 was digested at 37°C for 18 h with two methylation-sensitive enzymes, *Hpa*II and *Hha*I. PCR was performed using digested and undigested DNA with HUMARA primers (FAM-labeled ARf: 5'-TCCAGAATCTGTTCCAGAGCGTGC-3'; ARr: 5'-CTCTACGATGGGCTTGGGGAGAAC-3'). DNA fragment analysis was performed on an ABI3130xl autosequencer (Life Technologies). Fragment data were analyzed with GENEMAPPERT SOFTWARE version 4.1 (Life Technologies).

Results

Exome sequencing

Because this disorder was assumed to be an 'X-linked recessive' disorder based on the initial pedigree information, we focused on the X chromosome. Approximately 4.5 Gb of sequence data were generated, 87.3% of which was mapped to the human reference genome (UCSC hg19, NCBI build 37.1). MAQ was able to align 53,242,972 reads to the whole genome.

Two informatics methods identified 17 potential pathogenic changes (15 missense mutations, 1 nonsense mutation, and 1 splice-site mutation) (Table 1). The nonsense mutation was a false positive and all 13 missense mutations were inconsistent with the phenotype (no co-segregation). The mutation c.2388+1G>C was identified at the splice-acceptor site of intron 17 in *OFD1*, heterozygously in II-2, and hemizygotously in III-5, but was absent in II-3, III-3, and III-6 (Fig. 3a) as well as 93 normal female controls (0/186 alleles).

RT-PCR, direct sequencing

To examine the mutational effects of c.2388+1G>C, reverse transcriptase-polymerase chain reaction (RT-PCR) was performed. Only a 239-bp PCR product (wild-type allele) was observed in healthy control individuals (Fig. 3b). By contrast, a longer 1364-bp product was detected in II-2. Sequencing of the 1364-bp product revealed that a 1125-bp sequence of intron 17 was retained, producing a premature stop codon at amino acid position 796 (Fig. 3b). These data indicate

Exome sequencing in a family with an X-linked lethal malformation syndrome

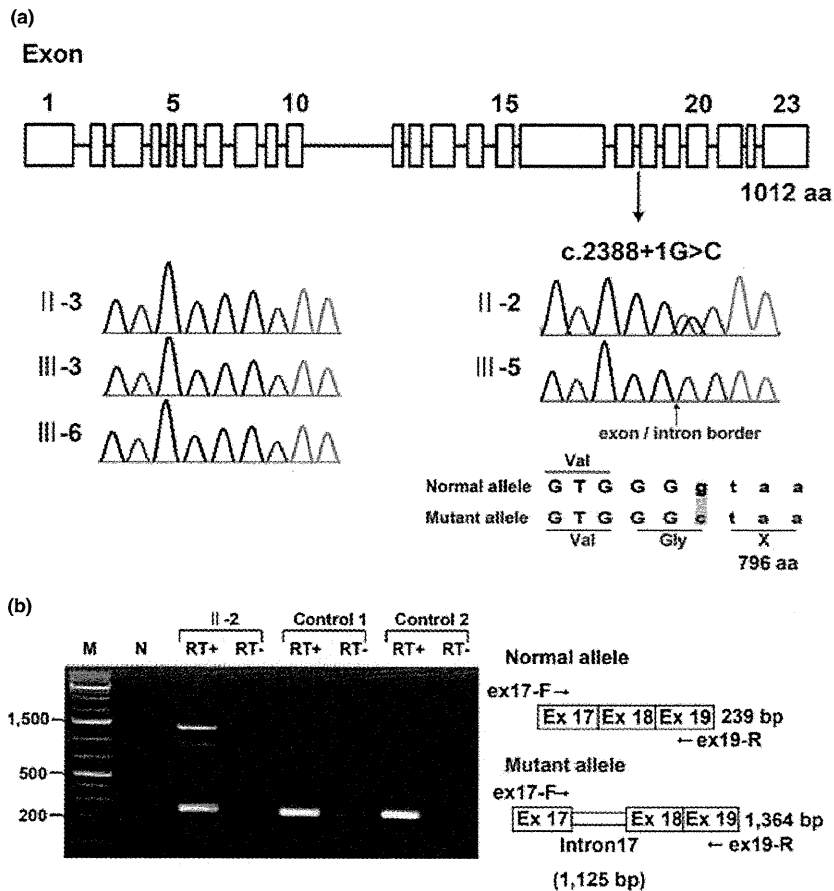


Fig. 3. (a) Gene structure of *OFDI* with the mutation (c.2388+1G>C) (upper). Electropherograms of the family members. Wild-type sequences are seen in II-3, III-3 and III-6. Heterozygous and hemizygous mutations are observed in II-2 and III-5, respectively. (b) Reverse transcriptase-polymerase chain reaction analysis showing both 239-bp and 1364-bp products in II-2, and only 239-bp products in two normal female controls. The 239-bp product is normal and the 1364-bp product is aberrant.

that the c.2388+1G>C mutation in *OFDI* is most likely the causal mutation in this family.

X-chromosome inactivation assay

X-chromosome inactivation patterns was random patterns in II-2 available for this study (ratio > 38:62).

Discussion

Exome sequencing detected a single-base substitution (c.2388+1G>C) in *OFDI*, resulting in an error in splicing of intron 17 and a premature stop codon at amino acid position 796, in an affected male (III-5) and a carrier female (II-2) in this family with an 'unclassified' X-linked lethal congenital malformation syndrome. II-4 and III-1, who had strikingly similar clinical manifestations to III-5, are likely to have had the same *OFDI* mutation as III-5, although their DNA was not available. Through reassessment of clinical features of the family, the three affected males shared facial, oral, and digital malformations characteristic of OFD1 (4). Additionally, they exhibited more severe

complications in various systems including congenital heart defects, genitourinary malformations, and ophthalmological abnormalities. II-2 was also found to have subtle features of OFD1 (accessory frenulae and irregular teeth). Thus, we have concluded that the 'unclassified' X-linked lethal congenital malformation syndrome in this family was clinically compatible with OFD1.

An *OFDI* mutation (c.2123_2126dupAAGA in exon 16, p.Asn711Lysfs*3) was also detected in a family with an X-linked recessive mental retardation syndrome (10). Nine affected males had macrocephaly and severe mental or developmental retardation, and suffered from recurrent respiratory tract infections leading to early death in eight. Only an 11-year-old boy survived with severe mental retardation (IQ 20), obesity, and brachydactyly. His younger brother had postaxial polydactyly. No cognitive, oral, facial, digital, or renal abnormalities were detected in heterozygous carrier females in that family. The patients were later classified into an infantile lethal variant of Simpson-Golabi-Behmel syndrome (type 2) (SGBS2, OMIM #300209), which had consisted of only one family,

genetically mapped to Xp22, including four maternally related affected males with hydrops at birth, craniofacial anomalies (macrocephaly, low-set posteriorly angulated ears, hypertelorism, short and broad nose with anteverted nares, large mouth with thin upper vermilion border, prominent philtrum, high-arched or cleft palate, and short neck), redundant skin, hypoplastic nails, skeletal defects involving upper and lower limbs, gastrointestinal and genitourinary anomalies, hypotonia and neurological impairment, and early death within the first 8 weeks (11, 12). Other *OFD1* mutations were detected in two families with Joubert syndrome-10 (JBTS10, OMIM #213300) (13). A mutation (c.2844_2850delAGACAAA in exon 21, p.Lys948Asnfs*9) in a family with eight affected males caused severe mental or developmental retardation and recurrent infections in all; postaxial polydactyly in five, retinitis pigmentosa in three, and a molar tooth sign on brain magnetic resonance imaging (MRI) in two. No heterozygous carrier females had any symptoms similar to those in the affected males. Another mutation (c.2767delG in exon 21, p.Glu923Lysfs*4) was found *de novo* in a 12-year-old male patient with severe mental retardation, macrocephaly, obesity, postaxial polydactyly, and a molar tooth sign on brain MRI (13).

To discuss whether these male patients with hemizygous truncating *OFD1* mutations would have different conditions (OFD1, SGBS2, or JBTS10) or belong to the same syndrome spectrum, we have created a comprehensive list of clinical manifestations in all of them (Table 2) (7, 10, 13). Macrocephaly, polydactyly (postaxial), respiratory insufficiency with recurrent respiratory tract infections in survivors, and severe mental or developmental retardation were shared by all the families (7, 10, 13). Nasal bridge features (depressed or broad) and lip abnormalities (cleft lip, pseudocleft lip, full lips, and prominent philtrum) were shared by the families with OFD1 and JBTS10 (7, 13). Brain malformations including hypoplasia or agenesis of corpus callosum, hypoplasia or agenesis cerebellar vermis as well as posterior fossa abnormalities (large, occipital encephalocele) were also shared by the families with OFD1 and JBTS10 (7, 13). III-5 in the present family was described to have Dandy-Walker malformation on brain ultrasonography. Three patients with JBTS10 were described to have a molar tooth sign on brain MRI, which is the characteristic neuroradiological hallmark of Joubert syndrome (13). Dandy-Walker malformation, typically consisting of agenesis or hypoplasia of cerebellar vermis, a cystic dilatation of the fourth ventricle, and an enlarged posterior fossa with a high position of the tentorium, is usually distinguishable from Joubert syndrome, characterized anatomically by agenesis or hypoplasia of cerebellar vermis and enlargement of the superior cerebellar peduncles and deep interpeduncular fossa resulting from a lack of normal decussation of superior cerebellar peduncular fiber tracts, leading to the characteristic 'molar tooth' appearance on transverse computed tomography and MRI of the mid-brain (14); and clinically by hypotonia, developmental

retardation, abnormal respiratory patterns, and oculomotor apraxia (15). However, Joubert syndrome could be present in association with Dandy-Walker malformation (15); and in such a case, Dandy-Walker malformation was reported to have initially masked the molar tooth sign because of a cystic dilatation of the fourth ventricle (16). Some authors state that the presence of the molar tooth sign does not, in itself, allow a diagnosis, Joubert syndrome, to be made; but that clinical evidence of the syndrome including hypotonia and developmental retardation accompanied by either abnormal breathing or abnormal eye movements should be present (14, 17). Typical respiratory abnormalities in Joubert syndrome, represented by short alternate episodes of apnea and hyperpnea or episodic hyperpnea alone (18), were not described in the patients with JBTS10, with only one presenting with stridor and intermittent cyanosis soon after birth (13). Abnormal eye movements including oculomotor apraxia were not mentioned in those with JBTS10 (13). In view of these evidences, it is reasonable to consider that the male patients with *OFD1* mutations, identified to date, would belong to a clinical continuum with wide intra- and inter-familial phenotypic variations of a single disorder.

A review by Macca and Franco (4) summarized all reported mutations in OFD1 patients. In total, 99 different mutations (7 genomic deletions and 92 point mutations) were identified, including 67 frameshift mutations (58%), 14 missense mutations (12%), 14 splice-site mutations (12%), 13 nonsense mutations (11%), and an in-frame deletion. Point mutations occur only in the first 17 exons (*OFD1* consists of 23 exons). A significant genotype-phenotype correlation between high-arched/cleft palate and missense and splice-site mutations has been identified (19). In addition, cystic kidney is more frequently associated with mutations in exons 9 and 12 (19). Quantitative PCR analysis of *OFD1* mRNA levels in EBV-LCLs from two families with JBTS10 showed that 30% and 58% of *OFD1* expression remained, suggesting that the mutant mRNA would be subject to nonsense-mediated decay and that the phenotypic variability observed for *OFD1* mutations would be caused by changes in activity of remaining truncated OFD1 protein (13). To date, premature stop codons at 713 in exon 16 (19), 796 in exon 17 (this report), 926 in exon 21 (13), and 956 in exon 21 (13) are associated with survival in males with hemizygous truncating *OFD1* mutations and no or subtle clinical manifestations in females with heterozygous *OFD1* mutations. Heterozygous truncating *OFD1* mutations preserving normal exons 1–16 have been reported in only two families with typical female OFD1 patients: a single-base deletion (c.2349delC in exon 17, p.Ileu784Serfs*85) (20) and a deletion of complete exon 17 (21). Mutations producing longer truncated protein (~ exon 17) might cause a milder form of the disorder that could not be detected in typical female OFD1 patients, but could be detected in male patients with multiple congenital anomalies and probable lethality in childhood.

Table 2. Clinical features of male patients with *OFD1* mutations

Patient	Family 1 (present family)			Family 2 ^b	Family 3 ^c				Family 4 ^d (W07-713)			Family 5 ^d (UW87)	Carrier
	II-4	III-1	III-5	1	IV-1	IV-3	IV-11	6 Patients	III-9	IV-10	6 Patients	(UW87)	19 Females
Age	0d/D	14d/D	1d/D		11 y	18 m/D	3 y/D	D	34 y	3.5 y	D (3)		
Birth weight (g) (gestational age)	2056 (33)	3064 (39)	1704 (32)		3850 (40)	4120 (38)	1915 (35)			3050 (Te)		4090 (41)	
Macrocephaly (>1.5 SD)	+		+		+	+	+	Some				+	
Obesity					+							+	
Craniofacial (87.3% ^a)									-	-	-		
Facial anomalies (69.1% ^a)													
Prominent forehead	+		+										
Redundant neck skin	+											+	
Hypertelorism	+	+	+	+									
Epicanthus		+											
Short palpebral fissures	+	+											
Nasal bridge features	Dep		Dep						Br	Br		Dep	
Low-set ears	+	+			+				+	+			
Lip abnormalities (32.6% ^a)	PCL	CL	PCL	PCL					FL, PP	FL, PP		PCL	PCL (1)
Oral													
Palatal abnormalities (49.6% ^a)	CSP	CP	CSP	CSP	HP								
Accessory frenulae (63.7% ^a)													+
Tongue abnormalities (84.1% ^a)	Nar											MG	Lob (3)
Teeth abnormalities (43.3% ^a)													lr (1)
Skeletal													
Short fingers/brachydactyly					+		+			-		+	
Postaxial polydactyly (3.7% ^a)	LtH	BiH		BiHRtBLT		RtH				BiHF	BiHF (4)	BiHLtF	
Preaxial polydactyly (19.3% ^a)	BiBrHx	BiF		BiBHx	BiBrT								
Respiratory													
Laryngeal anomalies	+												
Respiratory insufficiency	+	+				+	+		+	+		+	
Recurrent infections					+	+	+	+	+	+	+	+	
Cardiovascular													
Congenital heart defects	ASD, PDA	AVSD	HLHS	AVSD									
Genitourinary													
Cystic kidney	-		-		-	-			-	-	-	-	
Urinary tract abnormalities	HU	EUO											
Genital abnormalities	MP, C												
Gastrointestinal													
Esophageal abnormalities			+										
Ophthalmological													
Microphthalmia/microcornea	+												
Persistent papillary membrane		+											

Exome sequencing in a family with an X-linked lethal malformation syndrome

Table 2. Continued

Patient	Family 1 (present family)			Family 2 ^b	Family 3 ^c				Family 4 ^d (W07-713)			Family 5 ^d (UW87)	Carrier 19 Females
	II-4	III-1	III-5	1	IV-1	IV-3	IV-11	6 Patients	III-9	IV-10	6 Patients		
Optic disc coloboma		+											
Optic nerve atrophy													+
Retinal detachment	+												
Retinitis pigmentosa													
Central nervous system (48.4% ^a)													
Hydrocephalus		+	+	+	-	-	+						
Gyrus abnormalities	Hp			PM	-	-	-						
Corpus callosum abnormalities		Ag		Ag	-	-	-						Hp
Cerebellar vermis abnormalities		Ag	Ag		-	-	-		Hp	Hp			
Thick superior cerebellar peduncles					-	-	-		+	+			
Molar tooth sign					-	-	-		+	+			+
Dandy-Walker malformation			+		-	-	-						
Posterior fossa abnormalities				L	-	-	-			L			EC
Developmental/mental retardation					S	S	+	S	S	S	+	(All)	S

+, present; -, absent; blank, data not available; Ag, agenesis; ASD, atrial septal defect; AVSD, atrioventricular septal defect; BHx, bifid halluces; Bi, bilateral; BLT, bifid little toe; Br, broad; C, cryptorchidism; CL, cleft lip; CP, cleft palate; CSP, cleft soft palate; d, days; D, death; Dep, depressed; EC, encephalocele; EUO, ectopic urethral opening; F, foot/feet; FL, full lips; H, hand(s); HF, hands and feet; HLHS, hypoplastic left heart; Hp, hypoplasia; HP, high palate; HU, hydroureter; Hx, halluces; Ir, irregular; L, large; Lob, lobulated; Lt, left; m, months; MG, midline groove; MP, micropenis; Nar, narrowing of the tip of the tongue; PCL, pseudocleft of the upper lip; PDA, patent ductus arteriosus; PM, polymicrogyria; PP, prominent philtrum; Rt, right; S, severe; Te, term; T, thumbs; y, years.

^aFrom Macca and Franco (4).

^bFrom Goodship et al. (7).

^cFrom Budny et al. (10).

^dFrom Coene et al. (13).

Exome sequencing in a family with an X-linked lethal malformation syndrome

High-throughput, next-generation sequencing (NGS) has had a tremendous impact on human genetic research (22). Moreover, techniques enabling enrichment of selected regions enable us to use NGS efficiently and to identify the causative genes for a reasonable number of genetic disorders as well as susceptibility genes for complex diseases and health-related traits (23). In particular, X-linked disorders are good candidates for exome sequencing. We recently identified a nonsense mutation in *MCT8* causing X-linked leukoencephalopathy in a family from only two affected male samples (24). We have also identified two possible but inconclusive missense variants (*LICAM* and *TMEM187*) in a family with an atypical X-linked leukodystrophy from only two affected male samples (25). In this study, exome sequencing accompanied by appropriate bioinformatics techniques and a co-segregation evaluation successfully revealed a disease-causing mutation in *OFDI*, which could not have been assumed to be a candidate based on the clinical manifestations of the affected male patients. Unbiased rapid screening through these technologies is a powerful method for the detection of mutations in unexpected causative genes in undiagnosed patients with multiple congenital malformations.

In conclusion, we have identified a causative splicing mutation in *OFDI*, through exome sequencing, in a family with three males having an 'unclassified' X-linked lethal congenital malformation syndrome. The affected males manifested severe multisystem complications in addition to the cardinal features of OFD1 and the carrier female showed only subtle features of OFD1. The present patients, as well as the previously reported male patients from four families (one with clinical OFD1; one with *SGBS2* and an *OFDI* mutation; two with *JBTS10* and *OFDI* mutations), would belong to a single syndrome spectrum caused by truncating *OFDI* mutations, presenting with craniofacial features (macrocephaly, depressed or broad nasal bridge, and lip abnormalities), postaxial polydactyly, respiratory insufficiency with recurrent respiratory tract infections in survivors, severe mental or developmental retardation, and brain malformations (hypoplasia or agenesis of corpus callosum and/or cerebellar vermis and posterior fossa abnormalities).

Acknowledgements

The authors are grateful to the family for their participation in this study. The authors are also thankful to Prof Germana Meroni (Cluster in Biomedicine, Trieste) for mutation analysis of *MIDI1*, Dr Takeshi Futatani (Department of Pediatrics, Toyama Prefectural Central Hospital, Toyama, Japan), Dr Masahiko Kawabata (Department of Internal Medicine, Toyama Prefectural Central Hospital, Toyama, Japan), and Dr Akio Uchiyama (Department of Pathology, Toyama Prefectural Central Hospital, Toyama, Japan) for collecting clinical information; Dr Gen Nishimura (Department of Radiology, Tokyo Metropolitan Children's Medical Center) for helping radiological assessment; and Miss Junko Kunimi (Department of Medical Genetics, Shinshu University School of Medicine, Matsumoto, Japan) and Dr Shin-ya Nishio (Department of Otolaryngology, Shinshu University School of Medicine, Matsumoto,

Japan) for their technical assistance. This work was supported by research grants from the Ministry of Health, Labour and Welfare (T. K., Y. F., H. S., N. Mi., and N. Ma.), the Japan Science and Technology Agency (N. Ma.), the Strategic Research Program for Brain Sciences (N. Ma.) and a Grant-in-Aid for Scientific Research on Innovative Areas (Foundation of Synapse and Neuro-circuit Pathology) from the Ministry of Education, Culture, Sports, Science and Technology of Japan (N. Ma.), a Grant-in-Aid for Scientific Research from Japan Society for the Promotion of Science (N. Ma.), a Grant-in-Aid for Young Scientist from Japan Society for the Promotion of Science (H. S. and N. Mi.) and a grant from the Takeda Science Foundation (N. Mi. and N. Ma.). This work was performed at the Advanced Medical Research Center, Yokohama City University, Japan.

Y. T., H. D., H. S., and N. Mi. performed the genetic analysis; T. K., K. H., Y. N., K. W., and Y. F. evaluated clinical aspects of the family, recruited samples, and prepared them for the analysis. Y. T., T. K. and N. Ma. wrote the manuscript.

Ethics approval

The work was approved by the Yokohama City University (Faculty of Medicine) and the Shinshu University (School of Medicine). Patient consent was obtained.

References

1. Papillon-Leage M, Psaume J. Une malformation hereditaire de la muqueuse buccale: brides et freins anomaux. *Rev Stomatol* 1954; 55: 209–227.
2. Gorlin RJ, Psaume J. Orofaciodigital dysostosis: a new syndrome. A study of 22 cases. *J Pediatr* 1962; 61: 520–530.
3. Ferrante MI, Giorgio G, Feather SA et al. Identification of the gene for oral-facial-digital type I syndrome. *Am J Hum Genet* 2001; 68: 569–576.
4. Macca M, Franco B. The molecular basis of oral-facial-digital syndrome, type I. *Am J Med Genet C* 2009; 151C: 318–325.
5. Toriello HV, Franco B. Oral-facial-digital syndrome type I. In: Pagon RA, Bird TD, Dolan CR, Stephens K, Adam MP, eds. *GeneReviews at genetests: Medical Genetics Information Resource (database online)*. Seattle, WA: Copyright, University of Washington, 1993–2011, from <http://www.genetests.org>. Accessed on July 23, 2011.
6. Morleo M, Franco B. Dosage compensation of the mammalian X-chromosome influences the phenotypic variability of X-linked dominant male-lethal disorders. *J Med Genet* 2008; 45: 401–408.
7. Goodship J, Platt J, Smith R, Burn J. A male with type I orofacioidigital syndrome. *J Med Genet* 1991; 28: 691–694.
8. Fontanella B, Russolillo G, Meroni G. *MIDI1* mutations in patients with X-linked Opitz G/BBB syndrome. *Hum Mutat* 2008; 29: 584–594.
9. Nishimura-Tadaki A, Wada T, Bano G et al. Breakpoint determination of X;autosome balanced translocations in four patients with premature ovarian failure. *J Hum Genet* 2011; 56: 156–160.
10. Budny B, Chen W, Omran H et al. A novel X-linked recessive mental retardation syndrome comprising macrocephaly and ciliary dysfunction is allelic to oral-facial-digital type I syndrome. *Hum Genet* 2006; 120: 171–178.
11. Terespolsky D, Farrell SA, Siegel-Bartelt J, Weksberg R. Infantile lethal variant of Simpson-Golabi-Behmel syndrome associated with hydrops fetalis. *Am J Med Genet* 1995; 59: 329–333.
12. Brzustowicz LM, Farrell S, Khan MB, Weksberg R. Mapping of a new *SGBS* locus to chromosome Xp22 in a family with a severe form of Simpson-Golabi-Behmel syndrome. *Am J Hum Genet* 1999; 65: 779–783.
13. Coene KL, Roepman R, Doherty D et al. *OFDI1* is mutated in X-linked Joubert syndrome and interacts with *LCA5*-encoded lebercilin. *Am J Hum Genet* 2009; 85: 465–481.
14. McGraw P. The molar tooth sign. *Radiology* 2002; 229: 671–672.
15. Chance PF, Cavalier L, Satran D, Pellegrino JE, Koenig M, Dobyns WB. Clinical nosologic and genetic aspects of Joubert and related syndromes. *J Child Neurol* 1999; 14: 660–666.

Tsurusaki et al.

16. Sartori S, Ludwig K, Fortuna M et al. Dandy-Walker malformation masking the molar tooth sign: an illustrative case with magnetic resonance imaging follow-up. *J Child Neurol* 2010; 25: 1419–1422.
17. Barkovich AJ. Anomalies with cerebellar dysgenesis: vermian dysgenesis. In: Barkovich AJ, ed. *Pediatric neuroimaging*, 4th edn. Lippincott Williams & Wilkins, Philadelphia 2005: 391–396.
18. Brancati F, Dallapiccola B, Valente EM. Joubert syndrome and related disorders. *Orphanet J Rare Dis* 2010; 5: 20.
19. Prattichizzo C, Macca M, Novelli V et al. Mutational spectrum of the oral-facial-digital type I syndrome: a study on a large collection of patients. *Hum Mutat* 2008; 29: 1237–1246.
20. Thauvin-Robinet C, Cossée M, Cormier-Daire V et al. Clinical, molecular, and genotype-phenotype correlation studies from 25 cases of oral-facial-digital syndrome type 1: a French and Belgian collaborative study. *J Med Genet* 2006; 43: 54–61.
21. Thauvin-Robinet C, Franco B, Saugier-Verber P et al. Genomic deletions of *OFDI* account for 23% of oral-facial-digital type 1 syndrome after negative DNA sequencing. *Hum Mutat* 2008; 30: E320–E329.
22. Shendure J, Ji H. Next-generation DNA sequencing. *Nat Biotechnol* 2008; 26: 1135–1145.
23. Bamshad MJ, Ng SB, Bigham AW et al. Exome sequencing as a tool for Mendelian disease gene discovery. *Nat Rev Genet* 2011; 12: 745–755.
24. Tsurusaki Y, Osaka H, Hamanoue H et al. Rapid detection of a mutation causing X-linked leukodystrophy by exome sequencing. *J Med Genet* 2011; 48: 606–609.
25. Tsurusaki Y, Okamoto N, Suzuki Y et al. Exome sequencing of two patients in a family with atypical X-linked leukodystrophy. *Clin Genet* 2011; 80: 161–166.

SHORT COMMUNICATION

The diagnostic utility of exome sequencing in Joubert syndrome and related disorders

Yoshinori Tsurusaki¹, Yasuko Kobayashi², Masataka Hisano³, Shuichi Ito⁴, Hiroshi Doi¹, Mitsuko Nakashima¹, Hiroto Saito¹, Naomichi Matsumoto¹ and Noriko Miyake¹

Joubert syndrome (JS) and related disorders (JSRD) are autosomal recessive and X-linked disorders characterized by hypoplasia of the cerebellar vermis with a characteristic ‘molar tooth sign’ on brain imaging and accompanying neurological symptoms including episodic hyperpnoea, abnormal eye movements, ataxia and intellectual disability. JSRD are clinically and genetically heterogeneous, and, to date, a total of 17 causative genes are known. We applied whole-exome sequencing (WES) to five JSRD families and found mutations in all: either *CEP290*, *TMEM67* or *INPP5E* was mutated. Compared with conventional Sanger sequencing, WES appears to be advantageous with regard to speed and cost, supporting its potential utility in molecular diagnosis.

Journal of Human Genetics (2013) 58, 113–115; doi:10.1038/jhg.2012.117; published online 4 October 2012

Keywords: *CEP290*; exome sequencing; *INPP5E*; Joubert syndrome; molecular diagnosis; *TMEM67*

Joubert syndrome (JS) and related disorders (JSRD) are autosomal recessive and X-linked disorders characterized by hypoplasia of the cerebellar vermis with the characteristic neuroradiological ‘molar tooth sign’ and accompanying neurological symptoms including dysregulation of breathing pattern, ataxia and developmental delay. JSRD are classified into six subtypes: pure JS, JS with ocular defect, JS with renal defect, JS with oculorenal defects, JS with hepatic defect and JS with orofaciocaudal defects.¹ To date, 17 causative genes have been identified in JSRD: *INPP5E*,² *TMEM216*,³ *AH1*,⁴ *NPHP1*,⁵ *CEP290*,⁶ *TMEM67*,⁷ *RPGRIP1L*,⁸ *ARL13B*,⁹ *CC2D2A*,¹⁰ *OFD1*,¹¹ *TTC21B*,¹² *KIF7*,¹³ *TCTN1*,¹⁴ *TMEM237*,¹⁵ *CEP41*,¹⁶ *TMEM138*,¹⁷ and *C5ORF42*.¹⁸ Because of the clinical and genetic heterogeneity in JSRD, it can be very difficult to identify the causative mutations in individual cases.

We encountered five non-consanguineous Japanese families with JSRD (Figure 1a) and molar tooth sign was observed in all patients (Figures 1b–e, Supplementary Table 1). Peripheral blood samples were obtained from patients and their family members after written informed consent was given. To identify causative mutations, we performed whole-exome sequencing (WES) in five probands of the five families (one proband from each family). DNA was processed using the SureSelectXT Human All Exon 50 Mb library or V4 (51 Mb) library (Agilent Technologies, Santa Clara, CA, USA), and sequenced on a Genome Analyzer IIx sequencer (Illumina, San Diego, CA, USA) with 108 bp paired-end reads, or on a HiSeq2000 sequencer (Illumina) with 101 bp paired-end reads and 7 bp index reads.

Image analysis and base calling were performed by Illumina pipeline. Approximately 3.8–6.0 Gb of sequence data were mapped to the human reference genome (GRCh37.1/hg19) with Novoalign or Burrows-Wheeler Aligner. The mean depth of coverage was 55–125 reads, with 88–96% of all coding exons being covered by 5 × or more reads.

Out of all variants within exons and ±20-bp intronic regions from the exon–intron boundaries, those registered in dbSNP135, 1000 Genomes and ESP5400 and located within the segmental duplications were removed. Homozygous or compound heterozygous variants of 17 JSRD causative genes were then picked up. In patients 1, 2, 3 and 4 whose DNA was captured by the SureSelectXT Human All Exon 50 Mb library, ~90% of the entire coding regions in 13 of 17 causative genes were covered by 5 × reads or more. In patient 5 captured by the V4 (51 Mb) library, >90% of the coding region was covered by 5 × reads or more (Supplementary Table 2), indicating that the V4 library offered superior coverage to the SureSelectXT library around the regions of the JSRD genes.

All patients from the five families possessed novel compound heterozygous mutations or a homozygous mutation in known genes later confirmed by Sanger sequencing (Figure 1a): c.1862G>A (p.R621Q)/c.700dupC (p.L234Pfs*56) in *INPP5E* (9q34.3) for family 1; c.5788A>T (p.K1930*)/c.6012-12A>T in *CEP290* (12q21.32) for family 2; c.329A>G (p.D110G)/c.2322 + 5delG in *TMEM67* (8q22.1) for family 3; homozygous c.6012-12A>T in *CEP290* for family 4; and c.214G>T (p.E72*)/c.6012-12A>T in *CEP290* for family 5. No other variants within 17 known genes have been identified after excluding

¹Department of Human Genetics, Yokohama City University Graduate School of Medicine, Yokohama, Japan; ²Department of Pediatrics, Gunma University Graduate School of Medicine, Maebashi, Japan; ³Department of Nephrology, Chiba Children's Hospital, Chiba, Japan and ⁴National Center for Child Health and Development, Tokyo, Japan
Correspondence: Dr N Miyake, Department of Human Genetics, Yokohama City University Graduate School of Medicine, 3-9 Fukuura, Kanazawa-ku, Yokohama 236-0004, Japan.

E-mail: nmiyake@yokohama-cu.ac.jp

Received 31 July 2012; revised 3 September 2012; accepted 5 September 2012; published online 4 October 2012

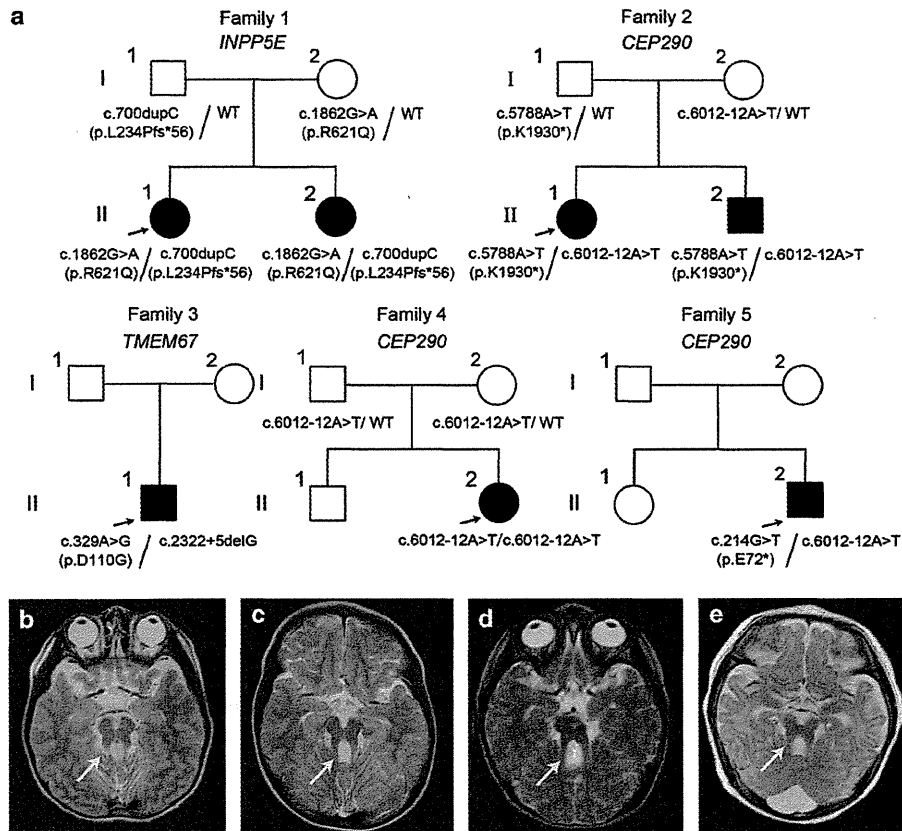


Figure 1 Familial pedigree and brain MRI of the patients. (a) JSRD families and mutations. (b) T2-weighted axial images of III-1, family 1. (c) T2-weighted axial images of III-2, family 1. (d) T2-weighted axial images of III-1, family 2. (e) T2-weighted axial images of III-2, family 2. The molar tooth sign is visible in all patients (arrowheads).

the variants of dbSNP135, 1000 Genomes and ESP5400. Clinical phenotypes caused by respective mutated genes are discussed in Supplementary text. In families 1, 2 and 4 in which parental samples were available, all parents were heterozygous carriers of one of the mutations. As parental samples were unavailable from families 3 and 5, we determined whether two mutations resided on different alleles by cloning a reverse transcriptase-PCR (RT-PCR) product amplified from total RNA of lymphoblastoid cells into a pCR4-TOPO vector (Life Technologies, Carlsbad, CA, USA) and sequencing. Each mutation was found in a different allele for both families (data not shown). Another variant, c.1894A>G (p.K632E) in *CEP290*, of family 2 was not found to be pathogenic based on web-based analyses such as SIFT, PolyPhen-2 and Mutation Taster (Supplementary Table 3). In families 2, 4 and 5 with a *CEP290* abnormality, c.6012-12A>T was shared. On the basis of our in-house 135 exome data, the allele frequency of the mutation was 1/270 allele (0.74%), indicating that it may be a rare variant in Japanese. The other mutations were not found in our in-house 135 exome data.

Splicing effects were examined in families 3 and 4. RT-PCR was performed on RNA from lymphoblastoid cells of family members using primers spanning exons 42/43 and 45/46 in family 4 and exons 20/21 and 24/25 in family 3 (sequence information available on request). In family 4, only an aberrant cDNA was detected in II-2, whereas the parents (I-1 and I-2) showed two different products including one wild-type, which was detected in a control

(Supplementary Figures 1a, b). Sequencing of the mutant product revealed a 57-bp insertion corresponding to the 3'-side of intron 43. As a result, a premature stop codon was introduced at intron 43. In family 3, RT-PCR detected a mutant cDNA in II-1 together with a wild-type product, which was detected in a control. Sequencing of the mutant product confirmed the skipping of exon 22, resulting in an in-frame 27 amino-acid deletion (Supplementary Figures 1c, d).

WES has proved a powerful tool for the identification of novel genes in genetic diseases. It also has tremendous potential for clinical diagnosis and is now being applied in the molecular diagnosis of single-gene disorders such as neurofibromatosis type 1, Marfan syndrome and multi-gene disorders such as retinitis pigmentosa.¹⁹ As shown here, WES would also be suitable for the diagnosis of JSRD, another multi-gene disorder. Though the read-coverage of the old version of SureSelect did not sufficiently collect genomic DNAs for four genes (*INPP5E*, *TMEM216*, *KIF7* and *TCTN1*), the performance of the V4 (51 Mb) library was satisfactory for all genes. Further, as exome capture technology is based on hybridization it can be refractory to homologous regions, so other methods such as multiplex PCR amplification and multiple microdroplet PCR technology could be useful in addition.

In conclusion, we were able to identify causative mutations in five non-consanguineous families with JSRD using WES. The diagnostic utility of WES is obvious, implying that WES or other next-generation sequencing technologies will be a main factor of molecular diagnosis.

ACKNOWLEDGEMENTS

We thank the patients and their families for their participation in this study. This work was supported by research grants from the Ministry of Health, Labor and Welfare (HS, N Matsumoto, N Miyake), the Japan Science and Technology Agency (N Matsumoto), the Strategic Research Program for Brain Sciences (N Matsumoto) and a Grant-in-Aid for Scientific Research on Innovative Areas-(Transcription cycle)-from the Ministry of Education, Culture, Sports, Science and Technology of Japan (N Matsumoto), a Grant-in-Aid for Scientific Research from Japan Society for the Promotion of Science (N Matsumoto), a Grant-in-Aid for Young Scientist from Japan Society for the Promotion of Science (HS, N Miyake) and a grant from the Takeda Science Foundation (N Matsumoto, N Miyake).

Web Resources: The URLs for data presented herein are as follows:

Novoalign, <http://www.novocraft.com/main/index.php>: Burrows-Wheeler Aligner, <http://bio-bwa.sourceforge.net/>: SIFT, <http://sift.jcvi.org/>: PolyPhen-2, <http://genetics.bwh.harvard.edu/pph2/>: Mutation Taster, <http://neurocore.charite.de/MutationTaster/>

- 1 Brancati, F., Dallapiccola, B. & Valente, E. M. Joubert Syndrome and related disorders. *Orphanet. J. Rare Dis.* **5**, 20 (2010).
- 2 Bielas, S. L., Silhavy, J. L., Brancati, F., Kisseleva, M. V., Al-Gazali, L., Sztriha, L. *et al.* Mutations in INPP5E, encoding inositol polyphosphate-5-phosphatase E, link phosphatidylinositol signaling to the ciliopathies. *Nat. Genet.* **41**, 1032–1036 (2009).
- 3 Valente, E. M., Logan, C. V., Mougou-Zerelli, S., Lee, J. H., Silhavy, J. L., Brancati, F. *et al.* Mutations in TMEM216 perturb ciliogenesis and cause Joubert, Meckel and related syndromes. *Nat. Genet.* **42**, 619–625 (2010).
- 4 Ferland, R. J., Eyaid, W., Collura, R. V., Tully, L. D., Hill, R. S., Al-Nouri, D. *et al.* Abnormal cerebellar development and axonal decussation due to mutations in AH11 in Joubert syndrome. *Nat. Genet.* **36**, 1008–1013 (2004).
- 5 Parisi, M. A., Bennett, C. L., Eckert, M. L., Dobyns, W. B., Gleeson, J. G., Shaw, D. W. *et al.* The NPHP1 gene deletion associated with juvenile nephronophthisis is present in a subset of individuals with Joubert syndrome. *Am. J. Hum. Genet.* **75**, 82–91 (2004).
- 6 Valente, E. M., Silhavy, J. L., Brancati, F., Barrano, G., Krishnaswami, S. R., Castori, M. *et al.* Mutations in CEP290, which encodes a centrosomal protein, cause pleiotropic forms of Joubert syndrome. *Nat. Genet.* **38**, 623–625 (2006).
- 7 Baala, L., Romano, S., Khaddour, R., Saunier, S., Smith, U. M., Audollent, S. *et al.* The Meckel-Gruber syndrome gene, MKS3, is mutated in Joubert syndrome. *Am. J. Hum. Genet.* **80**, 186–194 (2007).
- 8 Arts, H. H., Doherty, D., van Beersum, S. E., Parisi, M. A., Letteboer, S. J., Gorden, N. T. *et al.* Mutations in the gene encoding the basal body protein RPGRIP1L, a nephrocystin-4 interactor, cause Joubert syndrome. *Nat. Genet.* **39**, 882–888 (2007).
- 9 Cantagrel, V., Silhavy, J. L., Bielas, S. L., Swistun, D., Marsh, S. E., Bertrand, J. Y. *et al.* Mutations in the cilia gene ARL13B lead to the classical form of Joubert syndrome. *Am. J. Hum. Genet.* **83**, 170–179 (2008).
- 10 Gorden, N. T., Arts, H. H., Parisi, M. A., Coene, K. L., Letteboer, S. J., van Beersum, S. E. *et al.* CC2D2A is mutated in Joubert syndrome and interacts with the ciliopathy-associated basal body protein CEP290. *Am. J. Hum. Genet.* **83**, 559–571 (2008).
- 11 Coene, K. L., Roepman, R., Doherty, D., Afroz, B., Kroes, H. Y., Letteboer, S. J. *et al.* OFD1 is mutated in X-linked Joubert syndrome and interacts with LCA5-encoded lebercilin. *Am. J. Hum. Genet.* **85**, 465–481 (2009).
- 12 Davis, E. E., Zhang, Q., Liu, Q., Diplas, B. H., Davey, L. M., Hartley, J. *et al.* TTC21B contributes both causal and modifying alleles across the ciliopathy spectrum. *Nat. Genet.* **43**, 189–196 (2011).
- 13 Dafinger, C., Liebau, M. C., Elsayed, S. M., Hellenbroich, Y., Boltshauser, E., Korenke, G. C. *et al.* Mutations in KIF7 link Joubert syndrome with Sonic Hedgehog signaling and microtubule dynamics. *J. Clin. Invest.* **121**, 2662–2667 (2011).
- 14 Garcia-Gonzalo, F. R., Corbit, K. C., Sirerol-Piquer, M. S., Ramaswami, G., Otto, E. A., Noriega, T. R. *et al.* A transition zone complex regulates mammalian ciliogenesis and ciliary membrane composition. *Nat. Genet.* **43**, 776–784 (2011).
- 15 Huang, L., Szymanska, K., Jensen, V. L., Janecke, A. R., Innes, A. M., Davis, E. E. *et al.* TMEM237 is mutated in individuals with a Joubert syndrome related disorder and expands the role of the TMEM family at the ciliary transition zone. *Am. J. Hum. Genet.* **89**, 713–730 (2011).
- 16 Lee, J. E., Silhavy, J. L., Zaki, M. S., Schroth, J., Bielas, S. L., Marsh, S. E. *et al.* CEP41 is mutated in Joubert syndrome and is required for tubulin glutamylation at the cilium. *Nat. Genet.* **44**, 193–199 (2012).
- 17 Lee, J. H., Silhavy, J. L., Lee, J. E., Al-Gazali, L., Thomas, S., Davis, E. E. *et al.* Evolutionarily assembled cis-regulatory module at a human ciliopathy locus. *Science* **335**, 966–969 (2012).
- 18 Srour, M., Schwartzenruber, J., Hamdan, F. F., Ospina, L. H., Patry, L., Labuda, D. *et al.* Mutations in C5ORF42 Cause Joubert Syndrome in the French Canadian Population. *Am. J. Hum. Genet.* **90**, 693–700 (2012).
- 19 Zhang, W., Cui, H. & Wong, L. J. Application of next generation sequencing to molecular diagnosis of inherited diseases. *Top. Curr. Chem.* (e-pub ahead of print 11 May 2012; doi:10.1007/128_2012_325).

Supplementary Information accompanies the paper on Journal of Human Genetics website (<http://www.nature.com/jhg>)

Whole-Exome Sequencing Identified a Homozygous *FNBP4* Mutation in a Family With a Condition Similar to Microphthalmia with Limb Anomalies

Yukiko Kondo,¹ Eriko Koshimizu,¹ Andre Megarbane,² Haruka Hamanoue,³ Ippei Okada,¹ Kiyomi Nishiyama,¹ Hirofumi Kodera,¹ Satoko Miyatake,¹ Yoshinori Tsurusaki,¹ Mitsuko Nakashima,¹ Hiroshi Doi,¹ Noriko Miyake,¹ Hirotomo Saito,¹ and Naomichi Matsumoto^{1*}

¹Department of Human Genetics, Yokohama City University Graduate School of Medicine, Kanazawa-ku, Yokohama, Japan

²Medcal Genetics Unit, St. Joseph University, Beirut, Lebanon

³Department of Obstetrics and Gynecology, Yokohama City University Graduate School of Medicine, Kanazawa-ku, Yokohama, Japan

Manuscript Received: 4 January 2013; Manuscript Accepted: 9 March 2013

Microphthalmia with limb anomalies (MLA), also known as Waardenburg anophthalmia syndrome or ophthalmocromelic syndrome, is a rare autosomal recessive disorder. Recently, we and others successfully identified *SMOCl* as the causative gene for MLA. However, there are several MLA families without *SMOCl* abnormality, suggesting locus heterogeneity in MLA. We aimed to identify a pathogenic mutation in one Lebanese family having an MLA-like condition without *SMOCl* mutation by whole-exome sequencing (WES) combined with homozygosity mapping. A c.683C>T (p.Thr228Met) in *FNBP4* was found as a primary candidate, drawing the attention that *FNBP4* and *SMOCl* may potentially modulate BMP signaling. © 2013 Wiley Periodicals, Inc.

Key words: microphthalmia with limb anomaly; homozygous mutation; *FNBP4*; *SMOCl*; whole-exome sequencing (WES)

INTRODUCTION

Microphthalmia with limb anomalies (MLA [OMIM #206920]), also known as Waardenburg anophthalmia syndrome or ophthalmocromelic syndrome, is a rare autosomal recessive disorder first described by Waardenburg in 1935. Approximately 90% of families with MLA patients are consanguineous [Garavelli et al., 2006]. In 2011, 25 families were clinically reviewed [Rainger et al., 2011]. Patients show anophthalmia (91.4%, mostly bilateral), lower limb postaxial oligodactyly (82.9%), syndactyly of metacarpals 4th–5th finger (57.1%), and learning disability (37.1%) [Rainger et al., 2011]. We and others successfully identified *SMOCl* causative for MLA [Abouzeid et al., 2011; Okada et al., 2011]. Of note, seven of 18 families did not show *SMOCl* abnormalities [Okada et al., 2011; Rainger et al., 2011], indicating the locus heterogeneity in MLA. In this report, we present the result of whole-exome sequencing (WES) in one *SMOCl*-negative family with a condition like MLA.

How to Cite this Article:

Kondo Y, Koshimizu E, Megarbane A, Hamanoue H, Okada I, Nishiyama K, Kodera H, Miyatake S, Tsurusaki Y, Nakashima M, Doi H, Miyake N, Saito H, Matsumoto N. 2013. Whole-exome sequencing identified a homozygous *FNBP4* mutation in a family with a condition similar to microphthalmia with limb anomalies.

Am J Med Genet Part A 161A:1543–1546.

CLINICAL REPORT

The Lebanese family with a condition like MLA was previously described in detail (Fig. 1A) [Megarbane et al., 1998; Hamanoue et al., 2009; Okada et al., 2011]. Briefly, the main clinical features affecting the patient (anophthalmia, syndactyly of 2nd–3rd fingers on the right hand, postaxial polydactyly on the right foot, and

Additional supporting information may be found in the online version of this article.

Grant sponsor: Ministry of Health, Labor and Welfare of Japan; Grant sponsor: Japan Society for the Promotion of Science; Grant sponsor: Japan Science and Technology Agency; Grant sponsor: Ministry of Education, Culture, Sports, Science and Technology; Grant sponsor: Takeda Science Foundation.

*Correspondence to:

Dr. Naomichi Matsumoto, Department of Human Genetics, Yokohama City University Graduate School of Medicine, Fukuura 3-9, Kanazawa-ku, Yokohama 236-0004, Japan. E-mail: naomat@yokohama-cu.ac.jp

Article first published online in Wiley Online Library

(wileyonlinelibrary.com): 23 May 2013

DOI 10.1002/ajmg.a.35983

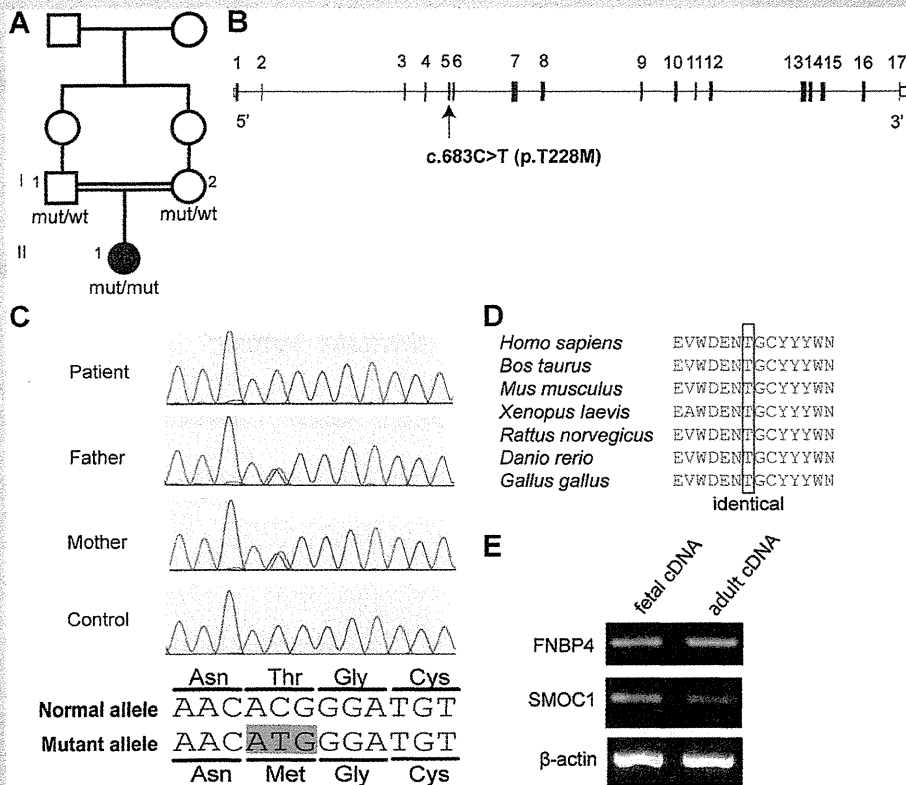


FIG. 1. Pedigree and *FBNP4* mutation and expression. **A:** Pedigree of the consanguineous MLA family. Black and open symbols denote affected and unaffected individuals, respectively. mut, mutant allele; wt, wild-type allele **[B]** Schematic representation of the *FBNP4*. UTR and coding region are open and filled rectangles, respectively. The location of the c.683C>T mutation is indicated by arrow. **C:** Electropherograms of the patient with a homozygous mutation (top), unaffected parents with a heterozygous mutation (middle) and a control with no mutation (bottom). A single nucleotide alteration in exon 5 caused an amino acid alteration. **D:** The missense mutation occurred at the evolutionally conserved amino acids. Homologous sequences were aligned using the CLUSTALW website [http://align.genome.jp/]. **E:** Expression analysis by PCR using human fetal and adult eye cDNA. *FBNP4*, *SMOC1* and β -actin were amplified.

bilateral ectrodactyly of the upper limbs) are somehow different from those of the classic MLA caused by *SMOC1* mutation (anophthalmia and limb anomalies such as postaxial oligosyndactyly).

GENETIC STUDIES

Genomic DNA was obtained from peripheral blood leukocytes using QuickGene 610-L (Fujifilm, Tokyo, Japan) after informed consent was given. DNA was amplified using GenomiPhi V2 kit (GE healthcare, Buckinghamshire, UK). Experimental protocols were approved by the Institutional Review Board of Yokohama City University School of Medicine. Seven anophthalmia-related genes (eTable SI—see Supporting Information online) were negative by Sanger sequencing. To check copy number variations (CNVs), the Genome-wide Human SNP Array 6.0 (Affymetrix, Santa Clara, CA) with Genotyping Console 3.0.1 (Copy Number Analyzer for GeneChip; Affymetrix) was used according to the manufacturer’s

instructions. No pathological CNVs were detected in the patient. Then, the SNP Array 6.0 data was also used for homozygosity mapping with HomozygosityMapper software [Bahlo and Bromhead, 2009]. A total of 14 >1-Mb homozygous regions were revealed, amounting to approximately 118.4 Mb in size and including 625 genes (eTable SII—see Supporting Information online). Among them, 14 candidate genes were negative by Sanger sequencing (eTable SI—see Supporting Information online).

WES was then performed. Three micrograms of DNA from the patient and his parents were processed using the SureSelect Human All Exon 50 Mb Kit (Agilent Technologies, Santa Clara, CA) or the SureSelect Human All Exon Kit v4 (51 Mb; Agilent) to generate exome libraries. The libraries were sequenced with an Illumina GAIx (Illumina Inc, San Diego, CA) or an Illumina HiSeq2000 (Illumina) with paired-end reads, according to the manufacturer’s instructions. Image analysis and base calling were performed by Sequence Control Software with Real-Time Analysis (Illumina) and

CASAVA software v1.7 (Illumina). Reads from GAIIX and Hiseq2000 were aligned and mapped to the human reference genome sequence (UCSC Genome Browser hg19, NCBI genome sequence website build 37) using Novoalign (Novocraft, Selangor, Malaysia; <http://www.novocraft.com/main/index.php>). Variant call as well as coverage and depth calculations were performed using the Genome Analysis Toolkit. Called single nucleotide variants (SNVs) were annotated with Annovar (Center for Applied Genomics, Children's Hospital of Philadelphia, Philadelphia, USA). Candidate variants were confirmed by Sanger sequencing with a 3130xL or 3500xL Genetic Analyzer (Applied Biosystems, Foster City, CA). The Human Gene Mutation Database (Biobases, Wolfenbuettel, Germany; <https://portal.biobase-international.com/hgmd/pro/start.php>) was used for checking whether the variants had been previously reported. PolyPhen-2 (<http://genetics.bwh.harvard.edu/pph2/>), SIFT (http://sift.jcvi.org/www/SIFT_BLink_submit.html), and MutationTaster (<http://www.mutationtaster.org/>) were used to evaluate variants in terms of sequence conservation, chemical change, and likelihood of pathogenicity. More than 85% of target regions were covered by 10 reads or more (eTable SIII—see Supporting Information online).

We adopted the following prioritization scheme to narrow down pathogenic mutations (Table I). First, we excluded the variants registered in the dbSNP135. In the trio (patient and parents) analysis, 844 SNVs of non-synonymous, canonical splice site change or small insertions or deletions were identified. Variants in segmental duplications or repeat elements registered in the Database of Genomic Variants (<http://projects.tcag.ac/variation/>) were excluded. Homozygous or compound heterozygous variants were picked up and confirmed by Sanger sequencing. Finally, five homozygous mutations and four heterozygous mutations remained, which were completely co-segregated with MLA (Table I). These variants were not found in the National Heart, Lung, and Blood Institute Exome Sequencing Project Exome Variant Server (5,400 exomes; <http://evs.gs.washington.edu/EVS/>), or our in-house 170 exomes. Among these, the homozygous mutation [c.683C>T (p.Thr228Met)] in *FNBP4* (NM_015308) is the primary candidate (Fig. 1A–C). The mutation occurred at the evolutionarily conserved amino acid among different species

(Fig. 1D). PolyPhen-2, SIFT, and MutationTaster indicate “probably damaging,” “pathogenic,” and “disease causing,” respectively. All the other homozygous and compound heterozygous variants were unlikely pathogenic based on the web-based analyses (eTable SI—see Supporting Information online).

Substantial *FNBP4* expression in eye tissues was confirmed by PCR using complementary DNA (cDNA) from human fetal and adult eye tissues (Biochain, Newark, CA; Fig. 1E). PCR mixture containing 2.5-ng cDNA, 1× ExTaq buffer, 2.5 mM each dNTP, 0.5 M each primer, and 0.25 U ExTaq HS polymerase (TakaraBio, Ohtsu, Japan) were cycled 35 times at 94°C for 30 sec, 60°C for 30 sec, and 72°C for 30 sec. β -Actin and *SMO1* (NM_001034852) were checked as positive controls. Primer information is available on request.

Knockdown experiments using zebrafish showed unexplained uniform early lethality with eye malformations which hamper appropriate evaluation partly due to small sizes (Supplemental eFig. 1—see Supporting Information online).

DISCUSSION

FNBP4 encodes formin binding protein 4 which interacts with FH1 domains in Formin1 (FMN1). Formin family proteins play as key regulators of actin and microtubule cytoskeletal dynamics during cell division and migration [Frazier and Field, 1997; Wasserman, 1998], but *FNBP4* function remains undetermined. This patient presents with ectrodactyly, which is exceptional in MLA. For normal limb development, three cell clusters including the apical ectodermal ridge (AER), the progress zone (PZ), and the zone of polarizing activity (ZPA) are of primary importance and produce signaling molecules determining the fate of neighboring cells by instructing them to remain undifferentiated, to proliferate, or to differentiate [Duijff et al., 2003]. Ectrodactyly is caused by error in the initiation and maintenance of the AER in the developing limb bud and disruption in signaling between the ZPA and the AER [Robledo et al., 2002]. Signals from the AER, including fibroblast growth factors, bone morphogenetic proteins (BMPs) and WNT signaling, allow the underlying mesenchymal cells of the PZ to maintain their proliferative activity, being modulated by Sonic

TABLE I. Sequence Variants Identified by Whole-Exome Sequencing

	Patient–parents trio	
	Novoalign/GATK/Annovar	
Total variant calls [not in dbSNP135]	1,414	
Variants not located in segmental duplications	1,115	
NS + SP + indels	844	
Candidate variants [AR model] [homozygous/compound heterozygous]	38/366	
Segregation confirmed genes [homozygous/compound heterozygous]	13/28	
Variants not found in 170 in-house exomes [homozygous/compound heterozygous]	5/4	
Predicted candidate genes to be pathogenic [homozygous/compound heterozygous]	1/0 <i>FNBP4</i> : c.683C>T [p.Thr228Met]	

GATK, Genome Analysis Toolkit; SNP, single nucleotide polymorphism; NS, non-synonymous variants; SP, canonical splice site variants; indels, small insertions or deletions. AR, autosomal recessive inheritance; SIFT, PolyPhen-2 and MutationTaster were used to predict the impact of an amino acid substitution on the structure and function of a human protein.